Marine Pollution Bulletin 129 (2018) 512–524

Contents lists available at ScienceDirect

Marine Pollution Bulletin

journal homepage: www.elsevier.com/locate/marpolbul

Assessing the effect of mercury pollution on cultured benthic foraminifera community using morphological and eDNA metabarcoding approaches

Fabrizio Frontalini[a,*], Mattia Greco[b], Letizia Di Bella[c], Franck Lejzerowicz[d], Emanuela Reo[d], Antonio Caruso[e], Claudia Cosentino[e], Antonella Maccotta[e], Giovanna Scopelliti[e], Maria Pia Nardelli[f], Maria Teresa Losada[g], Eric Armynot du Châtelet[h], Rodolfo Coccioni[a], Jan Pawlowski[d]

[a] Department of Pure and Applied Sciences, University of Urbino, 61029 Urbino, Italy
[b] MARUM, 28359 Bremen, Germany
[c] Department of Earth Science, Rome University "Sapienza", 00185 Roma, Italy
[d] Department of Genetics and Evolution, University of Geneva, 1211 Genève, Switzerland
[e] Dipartimento di Scienze della Terra e del Mare (DiSTeM), Università di Palermo, 90123 Palermo, Italy
[f] UMR CNRS 6112 LPG-BIAF, University of Angers, France
[g] Departamento de Zooloxía e Antropoloxía Física, Universidade de Santiago de Compostela, 27002 Lugo, Spain
[h] Univ. Lille, CNRS, Univ. Littoral Cote d'Opale, UMR 8187, LOG, Laboratoire d'Océanologie et de Géosciences, F 59 000 Lille, France

ARTICLE INFO

Keywords:
Benthic foraminifera
Mercury pollution
Metabarcoding
Biomonitoring

ABSTRACT

Mercury (Hg) is a highly toxic element for living organisms and is known to bioaccumulate and biomagnify. Here, we analyze the response of benthic foraminifera communities cultured in mesocosm and exposed to different concentrations of Hg. Standard morphological analyses and environmental DNA metabarcoding show evidence that Hg pollution has detrimental effects on benthic foraminifera. The molecular analysis provides a more complete view of foraminiferal communities including the soft-walled single-chambered monothalamiids and small-sized hard-shelled rotaliids and textulariids than the morphological one. Among these taxa that are typically overlooked in morphological studies we found potential bioindicators of Hg pollution. The mesocosm approach proves to be an effective method to study benthic foraminiferal responses to various types and concentrations of pollutants over time. This study further supports foraminiferal metabarcoding as a complementary and/or alternative method to standard biomonitoring program based on the morphological identification of species communities.

1. Introduction

Some heavy metals play an important role in cellular metabolism and growth but at high concentration they become toxic and pose serious threat to marine life (Stankovic et al., 2014). Heavy metals represent one of the most persistent pollutants in marine environment as they can be hardly degraded. Among them, mercury (Hg) is globally distributed in the atmosphere, in the geosphere (Gu et al., 2014) as well as in the biosphere where it is known to bioaccumulate and biomagnify as monomethylmercury(II) cation (CH_3Hg^+) (Gu et al., 2011). Mercury is subjected to physical, chemical and biochemical (i.e., biomobilization mediated by microorganisms) processes that condition its speciation and transport between the solid and aqueous phases (Fitzgerald et al., 2007; Gworek et al., 2016). In seawater, Hg occurs in different chemical and physical forms (Hines and Brezonik, 2004) influencing its bioavailability and toxicity (Batrakova et al., 2014). Total Hg concentration in the open ocean varies between 0.4 and 3 picomoles (pM) per liter (Lamborg et al., 2012; Mason et al., 2012). The Hg content in benthic sediments commonly reflects its level in the water (Gworek et al., 2016). In fact, Hg can be adsorbed on sediment particles, particularly on clay particles, and released as a result of chemical, physical and biological factors (Gworek et al., 2016). The toxicity of Hg depends on its concentration, chemical form and on the time of exposure (Ung et al., 2010; Scopelliti et al., 2015). Inorganic Hg has been considered toxic but at concentrations higher than methylmercury (Gentès et al., 2015). Therefore, the evaluation of the effects of this persistent pollutant in marine environments is of paramount importance and can be achieved with effective monitoring program based on reliable and comparable data as well as bioindicators. In this context, benthic foraminifera, single-celled organisms, are particularly sensitive to

* Corresponding author.
E-mail address: fabrizio.frontalini@uniurb.it (F. Frontalini).

http://dx.doi.org/10.1016/j.marpolbul.2017.10.022
Received 10 July 2017; Received in revised form 14 September 2017; Accepted 9 October 2017
Available online 14 October 2017
0025-326X/

ecological and environmental changes (for a review, Alve, 1995) and proved valuable as bioindicators in a wide range of marine environments (i.e., Frontalini and Coccioni, 2011). Although the majority of the field studies have highlighted the value of using benthic foraminifera in biomonitoring programs, the distinction between natural and human-induced stresses can sometimes be difficult to separate (Armynot du Châtelet and Debenay, 2010; Martins et al., 2015). In addition, there is a lack of information about quantitative pollutant-specific responses of foraminifera and only the effect of few contaminants has been considered so far. Under these circumstances, assessing the role played by a single pollutant, in the field, is undoubtedly a difficult task and the influence of additional factors on benthic foraminiferal assemblages cannot be ruled out (Frontalini and Coccioni, 2011). Laboratory experiments, through which benthic foraminiferal response to various types and concentrations of pollutants can be observed through time, represent the most effective and direct method to assess the effect of a single parameter (i.e., pollutant) on the benthic foraminiferal assemblages. Unfortunately, only a limited number of meso- and microcosm experiments have been conducted so far (i.e., Gustafsson et al., 2000; Ernst et al., 2006; Frontalini and Coccioni, 2012).

Traditional monitoring surveys based on morphological identification of benthic foraminifera are laborious, time-consuming and require highly trained specialists, sometimes making them costly and unsuitable for large-scale assessment (Pawlowski et al., 2014a, 2016). The introduction of high-throughput sequencing (HTS) technologies has stimulated the study of biodiversity from a molecular perspective (Metzker, 2010; Pawlowski et al., 2011; Creer et al., 2010; Baird and Hajibabaei, 2012), as testified by the dramatic accumulation of DNA barcodes in public databases (Pawlowski et al., 2012). The HTS of environmental DNA (eDNA) barcodes (metabarcoding) conveys useful information about benthic communities that result in consistent biotic indices calculations (Lejzerowicz et al., 2015), and therefore has presented an alternative method to assess the quality of marine environments (i.e., Pawlowski et al., 2016). The statistical developments and the extending application spectrum of this new tool provide enormous potential for the improvement of future environmental biomonitoring programs (Wood et al., 2013; Pawlowski et al., 2016; Cordier et al., 2017). Metabarcoding in environmental biomonitoring has been mainly applied to animals and marine macro-invertebrates and more recently to protists like foraminifera and diatoms (Visco et al., 2015; Pawlowski et al., 2016). Foraminiferal metabarcoding has been successfully applied for environmental monitoring of fish farming in Scotland (Pawlowski et al., 2014a), salmon farming in New Zealand (Pochon et al., 2015), oil drilling activity in New Zealand (Laroche et al., 2016), and characterizing microbial communities following the Deepwater Horizon event (Moss et al., 2016) but neither under laboratory controlled conditions nor heavy metal pollution.

Here, we analyze the diversity change of a benthic foraminiferal community cultured in mesocosm and exposed to selected concentrations of mercury (Hg). We compare the results of standard morphological analyses based on both Rose Bengal and CellTracker Green fixed foraminiferal assemblages with those from the HTS-based eDNA metabarcoding of foraminiferal community. We identify potential indicators of Hg pollution in molecular datasets and we discuss the advantages and limitations of metabarcoding compared to the standard morphology-based approach.

2. Materials and methods

2.1. Mesocosms and Hg concentrations

The collection site was a coastal area off the Mt. Conero (central Adriatic Sea) that is a natural area characterized by oligo-mesotrophic conditions, low influence of human activity and largely diversified benthic foraminiferal assemblages (Frontalini and Coccioni, 2008). Sediment was collected using a Van Veen grab sampler and only the top 2 cm of sediment was retained. Upon collection, sediments were homogenized and sieved over a 500 μm screen on board and the fraction > 500 μm was discarded to remove bioturbators such as macrofauna and large meiofauna. The < 500 μm fraction, containing foraminifera, was placed in an insulated box, covered by ambient seawater, and kept near ambient temperature (ca. 16 °C) until arrival at our shore-based laboratory. Artificial Sea Water (ASW) was prepared following the methods of Ciacci et al. (2012), stored in the dark, aerated and mixed under in-situ temperature. Seven different Hg-ASW mixture concentrations plus control were prepared. Inorganic salt of Hg as mercury chloride ($HgCl_2$) > 99.5% pure was used for the experiments (CAS Number 7487–94-7; Sigma-Aldrich). The selected final concentrations were 100 ppt, 1 ppb, 10 ppb, 100 ppb, 1 ppm, 10 ppm and 100 ppm plus the control. Approximately 20 L of Hg-ASW mixture was introduced into each tank (aquarium) (60 cm × 40 cm × 20 cm). Eight mesocosms (15 cm × 8 cm × 3 cm) containing 1 cm-thick sediment were placed inside each tank (Fig. S1). Multichannel pumps were used to circulate and to oxygenate water through silicone rubber tubing anchored between the tanks' bottom and plastic grids. Tanks were placed in a controlled environment with air temperatures of 14–16 °C that were uniformly maintained throughout the experiment. The dissolved oxygen (DO), salinity (S), conductivity, temperature (T), Oxidation-Reduction Potential (ORP) and pH of the seawater were routinely monitored by a set of HQ40d portable multi-parameter probes.

2.2. Subsampling

Mesocosms (sediment < 500 μm) were retrieved at six time intervals (one week (T1), two weeks (T2), three weeks (T3), four weeks (T4), six weeks (T5), and eight weeks (T6)). From each mesocosm and at every sampling time, 10 cm^3 of sediment was collected for morphological analyses based on Rose Bengal and CellTracker Green CMFDA (5-chloromethylfluorescein diacetate) dying (CTG) and a further aliquot (40 cm^3) of sediment was taken for geochemical analysis. For metabarcoding, three test sediments samples from original sampling and one sediment aliquot of 2 mL collected at every sampling time (except T4) were immersed in 5 mL of LifeGuard Soil Preservation Solution (MoBio) and immediately frozen at − 20 °C. Sterile gloves were worn at all time and disposable spoons were used for sub-sampling (SteriPlast, Burkle). A total of 43 sediment samples were sent frozen to the Department of Genetics & Evolution, University of Geneva (Switzerland) for further molecular work. Additionally, one aliquot (50 mL) of water was collected from tanks, immediately acidified with 50 μL of 65% nitric acid and refrigerated for the chemical analysis of Hg.

2.3. Hg analyses in water and sediment

The geochemical analyses of Hg in water and sediment were performed at the DiSTeM, Università di Palermo (Italy). Sediment samples were oven dried at low temperature (ca. 40 °C) for 48 h to prevent the evaporation of Hg and to remove porewater. Samples were then homogenized and reduced in powder using mortar and gently pestle. A fraction of about 0.2 g of the resultant materials was then weighted and digested in a microwave oven (Mars 5, CEM Corporation) using a mixed solution of HNO_3-H_2O_2-HF for a total digestion according to EPA method 3052. This procedure allows the complete decomposition of the organic material and the transformation of all the mercury in Hg(II). Milli-Q water (resistivity of 18.2 MΩ·cm) used throughout the experiments was produced by a Millipore system. Trace metal grade concentrated nitric and hydrofluoric acids and 30% hydrogen peroxide were purchased by Fluka. The digested samples were then filtered and brought to volume in a round-bottomed flask (50 mL). For each mineralization cycle 10 samples, a blank and a quality control sample (MESS-3, National Research Council Canada) were prepared. Subsequently, the samples were stored at 4 °C until the quantification of Hg

concentrations.

Mercury concentrations were measured by cold vapor atomic absorption spectroscopy (CV-AAS) using a flow injection system (FIAS 100, Perkin Elmer) connected to an atomic absorption spectrophotometry (AAS Analyst 800, Perkin Elmer). The sample solution, containing ionic Hg, was mixed with sodium borohydride (NaBH4) as reducing agent and HCl as carrier solution to form elemental Hg vapor. An inert carrier gas (argon) transported the Hg vapor in the detection cell where it was quantified at the wavelength of 253.7 mm. The quantification analysis was carried out using the direct determination by calibrated line built on three known concentration solutions. The unknown concentration was then calculated using the equation resulting from the linear regression. Three replicates of each measurement were performed. One blank and one digested standards were run every 10 samples to ensure the accuracy of digestion and analytical procedures. A relative standard deviation (RSD) below 5% was found for all of the samples analyzed. The instrument was recalibrated daily.

Correlation coefficients of the calibration curves were in the range of 0.998–0.999. The analytical results of the standard reference materials showed good agreement with the certified values. All data were blank corrected. The concentration of Hg in the sediment was related to the initial quantity of weighted samples.

2.4. Foraminiferal morphospecies assemblage

Aliquots treated with rose Bengal were gently washed through 63 μm sieve to remove any excess stain, and were then oven dried at 50 °C. One sample out of three was used for benthic foraminiferal counts that were separately performed on 63–125 μm fraction and > 125 μm fraction.

The sediment aliquots sampled for the CTG were immediately treated with a CTG/Dimethyl sulfoxide (DMSO) solution (Bernhard and Bowser, 1996). Overall, ca. 10 μL of the CTG/DSMO (1 μM final concentration) solution and 10 mL of ASW were added to the sediment (10 cm^3) aliquot with a micropipette. The sediments were incubated at in situ temperature (c.a. 15 °C) in the dark for 12 h. Samples were then fixed in 4% borax-buffered (5 g/L) formalin. The formalin-fixed sediment samples were washed with tap water to eliminate formalin and mud on a 63 μm sieve. The sediment samples were subsequently sieved over 125 and 63 μm meshes. Benthic foraminiferal counts were separately performed on 63–125 μm fraction and the > 125 μm fraction under an epifluorescence stereomicroscope (Stereo Discovery V8, Zeiss) equipped with a light fluorescent source (FITC LED 69). Samples were excited at a wavelength of 492 nm, whereas emission takes place at 517 nm (FITC). Only specimens showing clear green fluorescence have been wet picked and air-dried.

The benthic foraminifera were morphologically identified following classification of Loeblich and Tappan (1987), Jorissen (1988), Cimerman and Langer (1991), Fiorini and Vaiani (2001), and Frontalini and Coccioni (2008).

2.5. Environmental DNA metabarcoding

2.5.1. Environmental DNA extraction and PCR amplification

The total eDNA content of sediment was extracted for each of the 43 samples using the Power Soil™ DNA Isolation Kit (MoBio) according to the manufacturer instructions. All extractions were performed in a PCR-free environment, and in five separate sessions involving 4 to 9 samples per session to prevent extraneous contaminations. Moreover, blank extractions (i.e. extraction assay without sediment) were included at a ratio of 1:3 for the first session and then at a ratio of 1:8 in order to control for (cross-)contamination events.

A DNA fragment encompassing both the foraminiferal-specific 37f and 41f hypervariable regions of the 18S rRNA gene was PCR-amplified from each eDNA extract, using foraminiferal-specific forward primer s14F1 (5′ - AAGGGCACCACAAGAACGC - 3′) and reverse primer s17 (5′ - CGGTCACGTTCGTTGC - 3′) (Table S1) (Pawlowski et al., 2002). The amplified fragment was about 350 base pairs long. An additional, nested PCR step was performed using tagged versions of the same primers to label the PCR products of each of our samples to a combination of tag sequences.

Every tag consists of a unique sequence of 8 nucleotides appended to the 5′-end of the specific amplification primer sequence (Table S2). None of the 8-nucleotide sequence position is homologous to its corresponding position in the conserved region of the foraminiferal template sequences (absolute anti-complementarity). The minimum pairwise edit distance among forward primer tags and among reverse primer tags is set to 3. No dinucleotide is allowed in any tag, and the base diversity is maximized in order to be able to select tag primer pair combinations increasing the evenness of the anti-complementary bases at each of the 8 sequenced tag positions. The choice of the tagged-primers combinations was made according to an optimized multiplexing design as recommended previously (Esling et al., 2015).

Three PCR replicates were carried out for each eDNA extract. Each PCR was performed in a total volume of 25 μl, including 1 Unit of Taq DNA polymerase (Roche), 2.5 μl of 10 × PCR Reaction Buffer (Roche), 0.2 mM of each dNTP, 0.2 μM of each primer, and approximately 10 ng of eDNA extract. The conditions for the first amplification consisted of a predenaturation step at 95 °C for melt the complex genomic DNA mixture, followed by 19 cycles of denaturation at 94 °C for 30 s, annealing at 50 °C for 30 s and extension at 72 °C for 1:30 min, followed by a final extension step at 72 °C for 5 min. From the first PCR products, 10 ng were used for the nested PCR. The nested PCR conditions consisted of predenaturation step at 95 °C for 1 min, followed by 14 cycles of denaturation at 94 °C for 30 s, annealing at 52 °C for 30 s and extension at 72 °C for 2 min, followed by a final extension step at 72 °C for 5 min. One PCR blank control without DNA was included at a ratio of 1:1, i.e. for each sample processed to control each tagged primer pair combination. All blank controls remained negative throughout the experiments.

2.5.2. Library preparation and high-throughput sequencing

The PCR products were purified using High Pure PCR Cleanup Micro Kit (Roche) and then quantified using the fluorometric quantitation method based on the Qubit HS dsDNA Kit (Invitrogen). The purified samples were pooled in equal amounts) and the total volume was concentrated using a Speed Vac (30 min at medium temperature).

The sequencing library was prepared using the reagents of the PCR-free TruSeq kit (Illumina) according to the manufacturer instructions. In this procedure, the PCR products were end-repaired and appended with an adenine (A-tailing step), ligated to the Illumina adapter and purified. The library was quantified by qPCR using the KAPA Library Quantification Kit according to the manufacturer instructions, and then loaded on the single lane of a MiSeq flow cell for a paired-end sequencing run of 2*250 cycles. The sequencing primary analysis was conducted by MCS2.2.0. Detailed explanations of the Illumina HTS process have been provided elsewhere (Kircher et al., 2011).

2.5.3. Sequence analyses

The quality filtering and paired-reads assembly of the raw sequencing data, as well as the abundance filtering, sequence assignment, clustering and diversity estimation were based on the FASTQ file using a pipeline written in C language for which a beta version is publicly available (github.com/esling/illumina-pipeline). The sequencing also included the three test samples that are part of the FASTQ raw data but were not further considered. Briefly, we filtered out the sequences containing at least one undetermined position (“N”), having an average Phred quality score below 30, an edit distance of > 3 and 2 with its closest reference forward (or reverse) primer and associated tag, respectively, and > 5 mismatches in an overlap region of at least 50 positions between the paired reads. The demultiplexing step was performed for each pair of assembled reads based on the combination of

tags associated to the forward and reverse primers, and according to the experimental design. The clustering and assignment steps involve a pre-clustering step based on the 30 positions of the 5′-end of the 37f hypervariable region based on which foraminiferal species can be determined (Pawlowski and Lecroq, 2010). This pre-clustering is followed by a complete linkage clustering based on the pairwise Needleman-Wunsch distances computed for the complete 37f sequences of each pre-cluster, using a floating taxon-specific threshold for each pre-cluster, as extensively described in Lejzerowicz et al. (2014) and Pawlowski et al. (2014b).

Because there is no universal solution to the filtering of HTS data and that the abundance of sequences may be related to the likelihood for a sequence to be genuine, three different datasets were generated corresponding to three different read abundance thresholds for the filtering od the dereplicated, unique sequences. The Filter 1 dataset comprises all sequences except the unique sequences that were represented throughout the entire dataset by only one sequence read. In Filter 10 and Filter 100 datasets all sequences represented in the entire dataset by < 10 or 100 reads, respectively, were removed. Prior to the taxonomic assignment and the OTU clustering, the filtered sequences were ordered according to their sequence read counts and the least abundant sequences were grouped to the more abundant ones with up to 4 edit differences in order to remove sequencing errors among the set of unique sequences. The resulting sequences were then clustered into OTUs and for each OTU, the sequence represented by the highest number of reads was assigned a taxonomy based on a manually-curated database comprising 1069 non-redundant foraminiferal species sequences, as described in Pawlowski et al. (2014a). Chimeric OTUs originating from the artificial recombination of different sequences during the PCR steps were detected using Uchime v.4.232 based both on comparisons of OTUs sequences among them or against the reference database, and every detected candidate OTU was removed from the dataset.

2.6. Biostatistical analyses

A total of 7 datasets were generated, namely two from Rose Bengal morphological analyses (fractions > 63 μm and > 125 μm), two from CTG morphological analyses (fractions > 63 μm and > 125 μm), and three from the molecular data (one for each abundance-based filter: Filter1, Filter10, Filter100). Diversity indexes including Shannon (H′) and Fisher α were calculated for each dataset using the "Diversity" function in the Past software (Hammer et al., 2001), log-transformed and then correlated (Spearman's rank correlation) with the concentrations of Hg in sediment and water using Statistica v.8.

The morphological dataset that showed the strongest negative correlations between diversity indexes and Hg concentrations was further used for non-metric Multi-Dimensional Scaling (nMDS). The nMDS ordination was based on Bray-Curtis dissimilarity matrix (fourth-root transformed) derived from relative abundance of taxa (> 1%).

The Filter10 dataset has been chosen for further statistical analyses of metabarcoding data as it limits the number of OTUs and particularly of unassigned OTUs compared to Filter 1 and has a higher number of OTUs and of assigned OTUs than Filter 100. This dataset was explored after standardization in terms of relative abundance of the identified OTUs in each sample. The relative abundances of the most abundant OTUs were correlated (Spearman's rank correlation) with the concentrations of Hg in water and sediment. The OTUs showing significant correlation greater than |0.40| with Hg sediment concentration were examined with R software (R Core Team, 2016) and only OTUs with a relative read abundance > 3% were considered for nMDS analyses. The nMDS ordination based on the Bray-Curtis dissimilarity was used to represent the original position of OTU assemblages at each of the Hg concentration in multidimensional space as accurately as possible using a reduced number of dimensions. On the ordination diagrams, fitted smooth surface for both concentration and time are plotted. The stress between the two dimensional space representations and predicted values from the regression was estimated with a Shepard plot, showing scatter around the regression between each pair of species distance against their original dissimilarities. Stress < 0.05 indicates an excellent representation in reduced dimensions, 0.05–0.1 is good, 0.1–0.2 is acceptable, and 0.2–0.3 provides a poor representation. Multivariate Regression Trees (MRT) (De'ath, 2002) analysis was based on OTUs' relative read abundances to explore the relationships between their density and the Hg concentration. Successive partition is defined by a threshold value or a state of one of the explanatory variables. The densities of the OTUs were first standardized using a chord distance (Legendre and Gallagher, 2001). The read abundances of selected OTUs were plotted against the Hg sediment concentrations and quantile regression splines were modelled on 3rd order smoothed regression curve. All the calculations were carried out using R software (R Core Team, 2016) by using the packages base, Vegan (Oksanen et al., 2016) for the nMDS and the standardization of the data and mvpart (De'ath, 2014) for the Multivariate Regression Trees.

3. Results

3.1. Physico-chemical parameters and Hg concentrations

Temperature and DO remained homogenous along the experiment and salinity and pH showed a steady weak increase (Table S3). The mean value of salinity registered during the period of the experiment was 37‰ and a slight steady increase of lower than 1‰ was observed through the experiment (Table S3). The DO in the tanks maintained a constant value around 9.43 mg/L along the experiment (Table S3). Temporal changes of Hg (release and absorption) in water and sediment, respectively, are reported in Fig. 1. According to the water chemical and sediment geochemical analyses, a significant decrease of Hg concentrations in water takes place in the first (T1) and second weeks (T2) of the experiment. Gradually, the Hg concentrations decrease up to four weeks (T4) where then they mostly stabilize. The decrease of Hg concentration in water is mirrored by a concurrent increase of Hg in the sediment that follows the same pattern but in the opposite direction. In particular, no significant rise of Hg concentration in sediment seems to occur before T4 (Table S3).

3.2. Morphological assemblages

In total, 7,963 specimens of living (Rose Bengal stained) benthic foraminifera were sorted and taxonomically identified. A total of 27 morphospecies was identified, the majority belonging to the order Rotaliida (multilocular calcareous tests). The RB-stained assemblage was largely dominated by *Ammonia parkinsoniana, Ammonia tepida, Aubygnina perlucida, Eggerelloides scaber, Elphidium advenum, Nonionella turgida* and *Virgulinella fragilis* (Tables S4 and S5). On the other hand, a total of 4,834 CTB-labelled benthic foraminiferal specimens belonging to 30 morphospecies were picked (Tables S6 and S7). The living assemblages were dominated by *A. parkinsoniana*, *A. tepida, A. perlucida* and *Bulimina elongata*. On average 159.8 ± 6.3 and 248.8 ± 11 (n = 32) specimens were identified as living with Rose Bengal labeling technique in > 125 μm and > 63 μm fractions, respectively. On the other hand, on average 129.8 ± 3.5 and 151.1 ± 4.3 (n = 32) CTG-labelled specimens resulted living in > 125 μm and > 63 μm fractions, respectively. Data from the analyses on > 63 μm and > 125 μm fractions of both Rose Bengal-stained and CTG-labelled foraminifera were separately treated for the calculation of diversity indexes.

3.3. Molecular assemblages (high-throughput sequencing data statistics)

The raw sequencing data was composed of 717,228 Illumina MiSeq reads for the 43 samples of the whole Hg contamination experiment. The stringent sequence filtering procedure resulted in the removal of

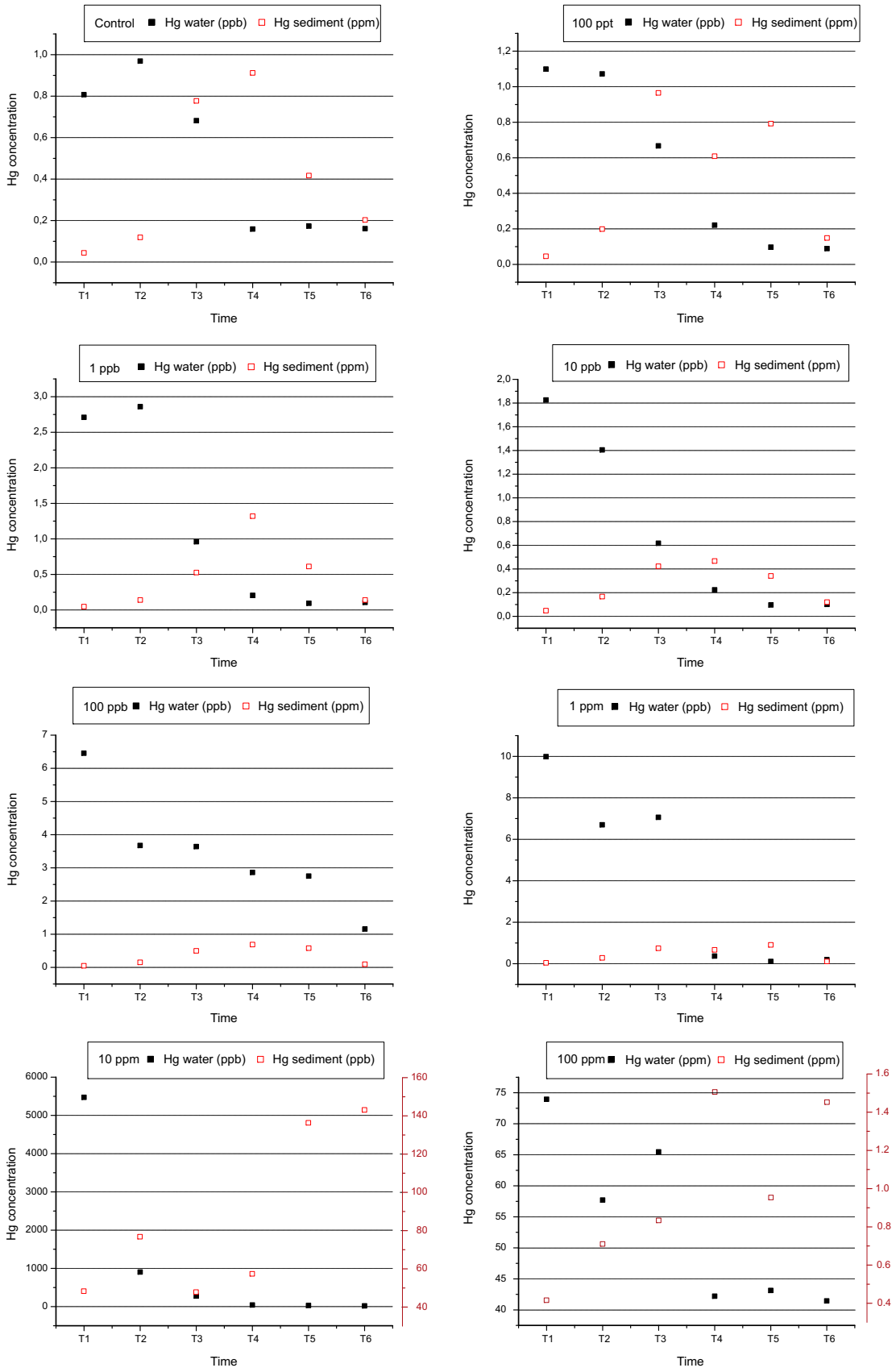

Fig. 1. Trend of Hg concentrations in water and sediment over time.

107,025 paired-end sequences (14.9%), because of low sequence quality (28,069 sequences), error in the primers or in the tags (65,635 sequences), mismatch in the overlap and failure to assemble the reads (7,374 sequences) and wrong tag primer combinations (5,947 sequences). Between 2,592 and 11,670 sequences were retained per sample, and c.a. 75% of the samples have > 5,240 sequences, which correspond to the first quartile of the numbers of sequences per sample (Table S8).

The filtered sequences were organized into three datasets, called filters 1, 10 and 100, depending on the fixed reads abundance threshold. The Filter 1 dataset was composed of 7,868 unique sequences that clustered into 1,048 OTUs (87% of them remained unassigned) (Tables S9). At threshold values of 10 or 100, the resulting dataset were reduced to 1,949 or 89 unique sequences, respectively. Filter 10 and Filter 100 datasets were composed of 430 and 56 OTUs, respectively (Tables S10 and S11). Each dataset was used to calculate diversity indexes but further analyses were based on Filter 10 only, which was composed on 150 OTUs assigned to Globothalamea (107 OTUs to Rotaliida and 43 OTUs to Textulariida), 119 OTUs assigned to Monothalamea, and 161 OTUs remained unassigned.

3.4. Foraminiferal response to Hg

3.4.1. Effect of Hg on foraminifera diversity

In all datasets generated both from the morphological and molecular analyses, the diversity decreased with increasing Hg concentrations in water and sediment. In both datasets, the diversity indexes (H′ and Fisher α index) were negatively correlated with the concentrations of Hg in water and sediment (Table 1), except for H′ calculated for the Rose Bengal > 125 μm in the case of Hg in sediment. These correlations are significant ($p < 0.05$) between diversity indices of molecular datasets corresponding to filters 1 and 10 and Hg concentrations in water and sediment. The Filter 100 dataset was significantly correlated only with Hg in water. In the case of morphological dataset, the significant negative correlation with Hg concentration was observed in few cases only. The highest negative values were observed for > 125 μm CTG-labelled foraminifera and Hg concentrations in sediment (− 0.36 for H′ and − 0.62 for Fisher α) and was therefore used for the further statistical analyses.

3.4.2. Effect of Hg on foraminiferal relative abundances (morphospecies)

The nMDS (stress 0.19) separates samples mostly following the Hg nominal gradient (Fig. 2A). In particular, samples with the lowest value of Hg concentration (control, 100 ppt, and 1 ppb) are mainly placed at negative values of the nMDS1 axis (Fig. 2A). These stations appear to be more diversified when compared to those samples located at positive values of nMDS1 (Fig. 2B). The strong dominance of *A. parkinsoniana* hampers the identification of relative abundances' changes of other taxa and only an increase of *A. parkinsoniana* and *A. tepida* compared to other species can be observed at the highest concentrations (100 ppm). The correlation matrix calculated to observe the changes of relative abundance of taxa to [Hg] variation depicts a negative significant correlation of *Bulimina marginata*, *Haynesina depressula*, *Nonion* cfr. *fabum*, V. *fragilis* and *Gavelinopsis* sp. with Hg. *Bulimina elongata* and *Elphidium advenum* appear to be positively related to Hg (Table S12).

Table 1
Spearman's rank correlation ($p < 0.05$) among diversity indexes (H′ and Fisher α index) calculated on morphological (Rose Bengal stained and CTG labelled benthic foraminifera in > 63 μm and > 125 μm fractions) and molecular (Filters 1, 10 and 100) datasets and Hg concentrations in water and sediment. Significant values are reported in bold.

Dataset	Diversity index	Hg water	Hg sediment
RB > 63 μm	H′	**0.56**	− 0.13
	Fisher α index	− 0.13	**− 0.44**
RB > 125 μm	H′	**− 0.52**	0.13
	Fisher α index	− 0.14	− 0.21
CTG > 63 μm	H′	− 0.07	− 0.14
	Fisher α index	− 0.28	**− 0.47**
CTG > 125 μm	H′	− 0.26	**− 0.36**
	Fisher α index	**− 0.36**	**− 0.62**
Filter 1	H′	**− 0.49**	**− 0.35**
	Fisher α index	**− 0.43**	**− 0.48**
Filter 10	H′	**− 0.39**	**− 0.42**
	Fisher α index	**− 0.31**	**− 0.44**
Filter 100	H′	**− 0.42**	− 0.12
	Fisher α index	**− 0.42**	− 0.13

3.4.3. Effect of Hg on foraminiferal relative abundances (eDNA data)

The relative abundances of the most abundant foraminiferal OTUs in Filter 10 dataset were correlated with the concentrations of Hg in water and sediment (Table S13). All the OTUs exhibited negative correlations with either Hg in water or sediment or both, except OTU 30 (unassigned monothalamid clone 87584), OTU 57 (Monothalamids Clade E, *Psammophaga*), OTU 6 (unassigned monothalamid), OTU 5 (Monothalamids Clade Y), OTU 7 (Rotaliida, Clade 3, *Virgulinella fragilis*) and OTU 1 (unassigned monothalamid).

The relative averaged abundances of OTUs were then plotted over the nominal Hg gradient (Fig. 3) where their positive or negative trend can be detected. Among analyzed OTUs, *Bathysiphon* (OTU 4), unassigned monothalamid (OTU 14), *Micrometula* sp. (OTU 13), unassigned monothalamid (OTU 17), *Leptohalysis* sp. (OTU 11), and *Psammophaga* sp. (OTU 21) exhibited a decreasing abundance towards higher Hg concentrations, particularly at 10 ppm and 100 ppm. On the other hand, unassigned monothalamid (OTU 1), monothalamid Clade Y (OTU 5) and unassigned monothalamid (OTU 29) appeared to be associated with increasing Hg concentrations. Similar results were achieved on the quantile regression spline (Fig. S2).

3.4.4. Identifying potential foraminiferal bioindicators in eDNA datasets

To further identify potential foraminiferal bioindicator species, the relative abundances of OTUs were analyzed using a nMDS (Fig. 4). As for the morphological data, the nMDS obtained for the eDNA data (stress 0.15) exhibits a separation among samples mostly following the Hg gradient. In particular, samples with the highest value of Hg concentration (10 and 100 ppm) were grouped together (Fig. 4A). Of the selected OTUs, with a relative abundance > 4%, unassigned monothalamids (OTU 1) and monothalamid Clade Y (OTU 5) showed an increase abundance at higher Hg concentrations (10 and 100 ppm), whereas *Bathysiphon* (OTU 4), *Micrometula* (OTU 13), unassigned monothalamid (OTU 26), *Leptohalysis* (OTU 11), *Psammophaga* (OTU 21), and Nonionidae Clade B (OTU 111) were only present or occurred in higher abundances at low Hg concentrations (Fig. 4A). The nMDS highlighted potential indicators OTUs (Fig. 4B). In particular, *Bathysiphon* (OTU 4), unassigned monothalamid (OTU 14), *Micrometula* (OTU 13), unassigned monothalamid (OTU 17), *Leptohalysis* (OTU 11), and *Psammophaga* (OTU 21) appeared to be negatively affected by increasing concentration of Hg. The OTUs that were associated with the highest values of Hg were unassigned monothalamid (OTU 1), monothalamid Clade Y (OTU 5) and Textulariida (OTU 15) (Fig. 4B).

On the basis of the OTUs' density, the MRT arranges the 40 samples in different clusters and subclusters (Fig. 5). The concentration is the primary discriminant variable. Accordingly, cluster 1 includes all the highest concentrations (10 ppm and 100 ppm) regardless the sampling time. Cluster 1 exhibits the highest abundances of unassigned monothalamid (OTU 1) and relative high abundances of monothalamid Clade Y (OTU 5). Cluster 2, which groups all the lower concentrations, is divided in two subclusters 2a and 2b, with the former including all the T5 and T6 time intervals regardless the concentrations. Cluster 2a shows the lowest of unassigned monothalamid (OTU 1).

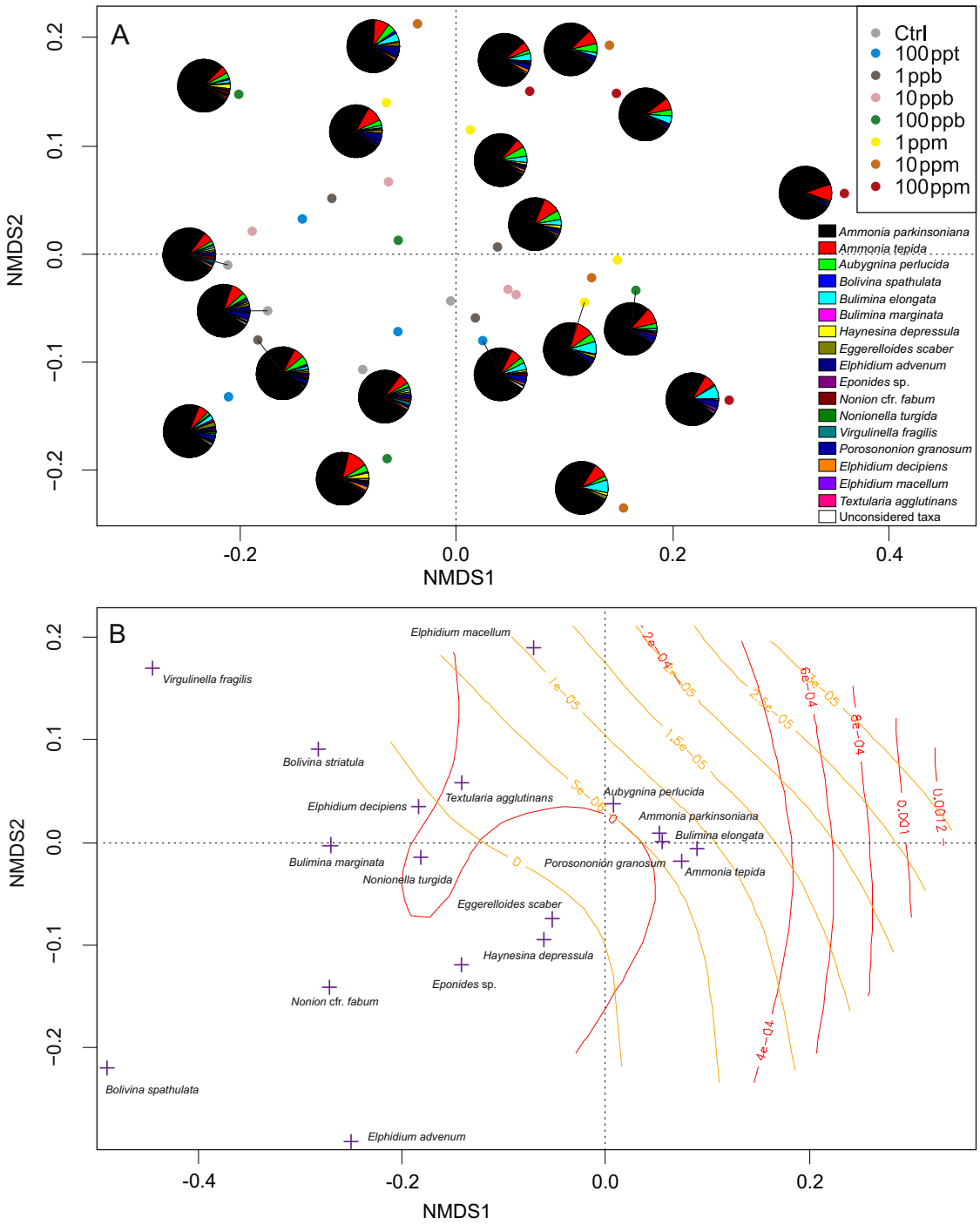

Fig. 2. Non-metric Multidimensional Scaling (NMDS) on the foraminiferal data (CTG > 125 μm) based on the Bray-Curtis dissimilarity matrix. (A) Plot of samples' concentrations and colored pie charts of selected samples represent the relative abundance of species (> 1% in abundance). (B) Plot of selected species as well as a fitted smooth surface for Hg initial concentration (orange) and Hg concentration in the sediment (red). (For interpretation of the references to color in this figure legend, the reader is referred to the web version of this article.)

4. Discussion

4.1. Mercury

In our experiment, $HgCl_2$ was chosen to evaluate the effect on the benthic foraminiferal assemblages. The delay in the Hg precipitation could be the reason why the concentration in the water of the 100 ppm tank appears to stabilize at about 42 ppm. In similar experiments, Maccotta et al. (2016) investigated the uptake of two heavy trace metal elements (Cr and Pb) in sediments and documented a comparatively different behaviors and kinetic for the two pollutants. In particular, at high concentrations (> 1 mg/L, that is 1 ppm), Cr absorption of sediment from seawater is twice faster than Pb likely due to differential metal ions' characteristics and their interaction with sediment (Maccotta et al., 2016).

The highest Hg measured concentrations in sediment (up to 1.5 ppm) in the present experiment were particularly high and can be compared with the values measured in sediment of the Santa Gilla (0.87 ppm on average up to 8.63 ppm), Venice (0.69 ppm on average and up to 4.28 ppm) and Orbetello (1.2 ppm on average and up to

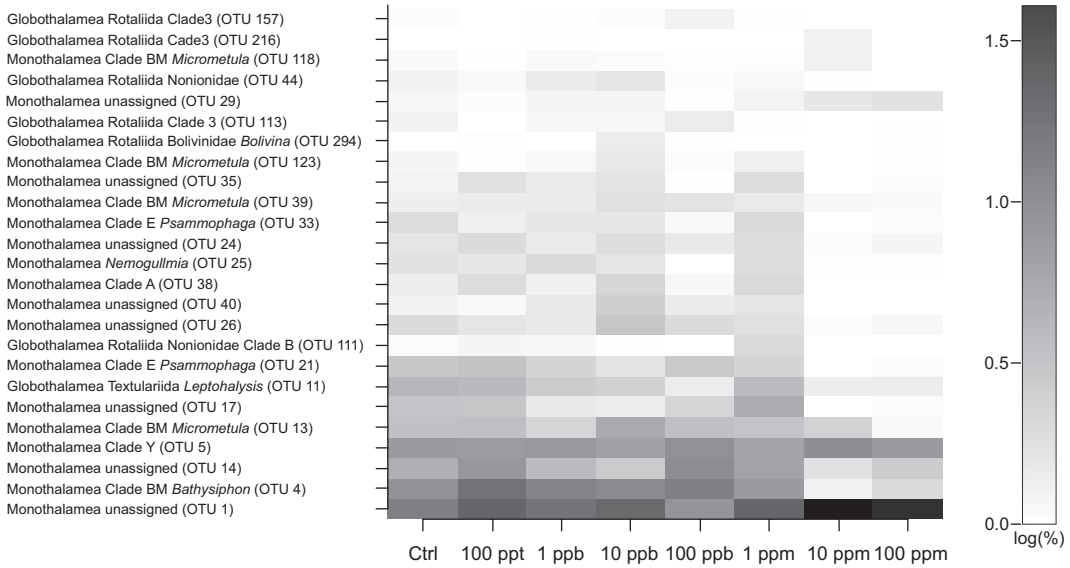

Fig. 3. Shade plot of the relative abundance of selected OTUs over nominal concentrations of Hg. Only OTUs with a Spearman's rank correlation > |0.40| with either sediment or water Hg concentrations were considered. Relative abundances of eDNA reads were logarithmically transformed.

2.64 ppm) lagoons (Coccioni et al., 2009; Frontalini et al., 2009, 2010) and much higher than those found in the Marche coastal area (30 ppb on average and up to 71 ppb) (Frontalini and Coccioni, 2008). The ERL (Effect Range Low) and ERM (Effect Range Median), which measure the toxicity in marine sediment, reported for the sediment guidelines of the U.S. Environmental Protection Agency (USEPA) for Hg (Long et al., 1995) are 150 ppb and 710 ppb, respectively. The ERM is defined as the concentration above which effects are frequently observed among most species of biota whereas the ERL as the concentration below which effects are rarely observed on biota (Long et al., 1995). The measured Hg concentrations in sediment exceed the ERM for all the 100 ppm nominal conditions except T1, whereas the ERL is overcome at 100 ppm T1 and is very close to 10 ppm at T5 and T6.

4.2. Benthic foraminiferal assemblages and Hg

The effects of Hg on benthic foraminifera have been documented by field studies, culture experiments and ultrastructural studies (i.e., Saraswat et al., 2004; Ferraro et al., 2006; Coccioni et al., 2009; Frontalini et al., 2009, 2016; Nigam et al., 2009). A diversity reduction and the development of abnormalities have been ascribed as the main effects of Hg on benthic foraminiferal assemblages (Ferraro et al., 2006; Coccioni et al., 2009; Frontalini et al., 2009; Caruso et al., 2011). Similar results were documented by Di Leonardo et al. (2007) through the study in vertical profiles of three box-cores from the industrial area of Augusta and the Palermo Gulf (Italy). Culture experiments on *Rosalina leei* revealed that increasing concentrations of Hg promote the inhibition of reticulopodial activity, the development of test abnormalities, slowdown of reproduction rate, as well as a growth reduction (Saraswat et al., 2004; Nigam et al., 2009). It was reported that regardless the concentrations after 40 days of exposure, *R. leei* ceased to grow but survived even at the highest concentration, namely 260 ng/L (Saraswat et al., 2004). The effect of sudden stress due to Hg was evaluated by Nigam et al. (2009) who reported specimens of *R. leei* dying at 300 ng/L after 19 days of exposure. At ultrastructural level, Hg has been suggested to promote the accumulation of lipid droplets and the proliferation of lysosomes (Frontalini et al., 2016). In the same study, the presence of Hg within the foraminiferal cell, namely at the basal part of pores, in the organic linings of the foramen/septa, and as cytoplasmic accumulations has been documented.

The concentrations of Hg used in the present study spans from 100 ppt to 100 ppm that cover and extend the range of concentrations considered by Saraswat et al. (2004) and Nigam et al. (2009). Differently from the culture experiments that directly exposed *R. leei* to Hg, our approach is based on the exposure of sediment and the entire foraminiferal assemblages living therein to Hg. Accordingly, the choice of very high concentrations (i.e., 10 ppm and 100 ppm) was to ensure still high Hg concentrations in seawater after partial absorption by the underlying sediment. Similar to field studies, increasing concentrations of Hg promote a reduction of diversity evaluated through a set of indexes (Shannon and Fisher α index). Interestingly, regardless the considerations of morphological and molecular analyses, a reduction of diversity has been observed. Comparatively more negative correlation values among diversity index and Hg concentrations are encountered in the CTG dataset than the Rose Bengal stained ones. Rose Bengal is a widely applied conventional staining technique to distinguish living from dead benthic foraminifera that has been extensively used in field studies (Murray, 2006). However, according to Bernhard et al. (2006), this non-vital stain might lead to a significantly overestimation of the abundance by including false positive (stained remaining proteins but not living specimens). On the other hand, the application of fluorogenic probes (i.e., CTG) is considered a more accurate method viability method (Bernhard et al., 2006). Both techniques have been considered in our experiment and a lower number of CTG-labelled specimens were recognized as living compared to RB-stained ones. The differences between density determinations using the two methods led to a 39.1% overestimation with Rose Bengal > 63 μm. This value matches quite well with the averaged one (47%) reported from Florida Margin and off the Carolinas (Bernhard et al., 2006). This bias can affect ecological studies (Bernhard et al., 2006) and even more significantly experimental ones. In light of this, the application of RB staining method should be used with care in laboratory experiments, particularly when short-time samplings (i.e., weeks) are compared. The relatively lower and mostly non-significant negative correlations of diversity indexes calculated in the Rose Bengal dataset with Hg in the sediment is possibly responsible to this bias.

Negative correlations with Hg concentration were also found for diversity indexes calculated in the eDNA datasets. Remarkably, the correlation values are more negative in the molecular datasets than in the morphological ones. A possible explanation might be found in the relatively poor diversification of the foraminiferal morphological assemblages when compared to the molecular ones. In fact, the low number of morphospecies identified in the RB (27) and CTG (30) data, were greatly outnumbered by the OTUs recognized in filters 1, 10 and

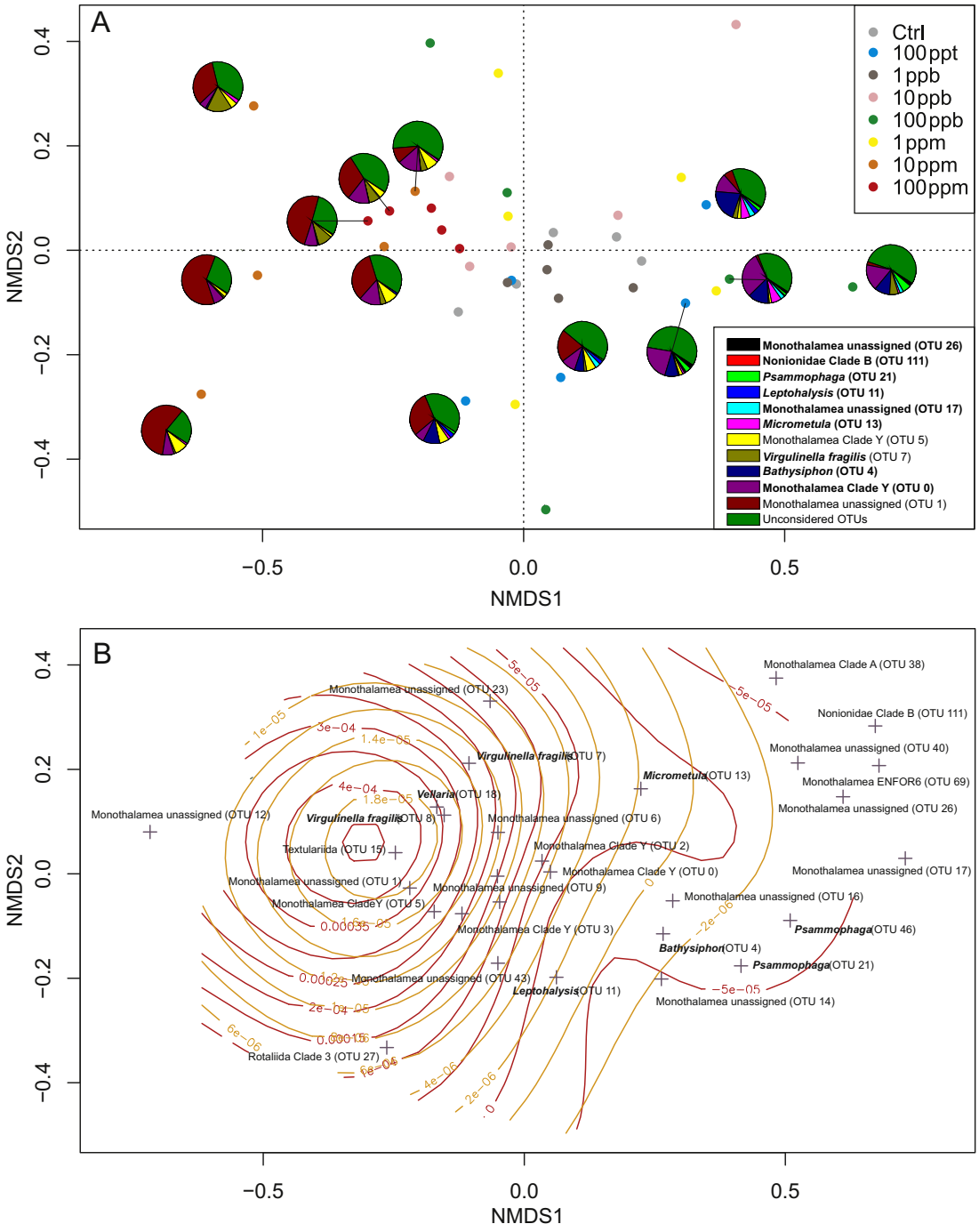

Fig. 4. Non-metric Multidimensional Scaling (NMDS) on the OTUs data of Filter 10 based on the Bray-Curtis dissimilarity matrix. (A) Plot of samples' concentrations and colored pie charts of selected samples represent the relative abundance of OTUs (> 4% in abundance). OTUs decreasing in relative abundance at higher concentrations are marked in bold while those increasing in relative abundance are not. (B) Plot of selected OTUs as well as a fitted smooth surface for Hg initial concentration (orange) and Hg concentration in the sediment (red). (For interpretation of the references to color in this figure legend, the reader is referred to the web version of this article.)

100 that account 1048, 430 and 56, respectively. Additionally, the foraminiferal morphological assemblages were strongly dominated by *Ammonia* species and specifically by *A. parkinsoniana* accounting for over 75%. The strong dominance of *A. parkinsoniana* in the morphological datasets hides therefore trends of variation of relative abundance of species (Fig. 2) and only some taxa that show very limited relative abundances (i.e., *B. marginata*, *H. depressula*, *Nonion* cfr. *fabum*, *V. fragilis* and *Gavelinopsis* sp.) have been putatively identified as sensitive to Hg increase. This dominance of *Ammonia* spp. was enhanced at higher Hg concentrations reflecting the poor diversification of foraminiferal assemblages. On the other hand, the eDNA (filters 1, 10 and 100) datasets that encompass all foraminiferal diversity, including monothalamiids, exhibited a wider number of OTUs (species) and were less dominated by few OTUs, making easier the recognition of possible sensitive OTUs easier. Interestingly, the separation of samples (concentration of Hg) for both morphological (CTG > 125 μm, Fig. 2) and molecular (Filter 10, Fig. 4) datasets was at concentrations over 10 ppm. This is particularly evident from the outcome of MRT analysis applied on molecular dataset (Fig. 5). After two weeks, the initial Hg concentrations of 100 ppm in water was still exceeding the ERM value (710 ppb) that is considered as the threshold over which significant effects on biota are frequently observed (Long et al., 1995).

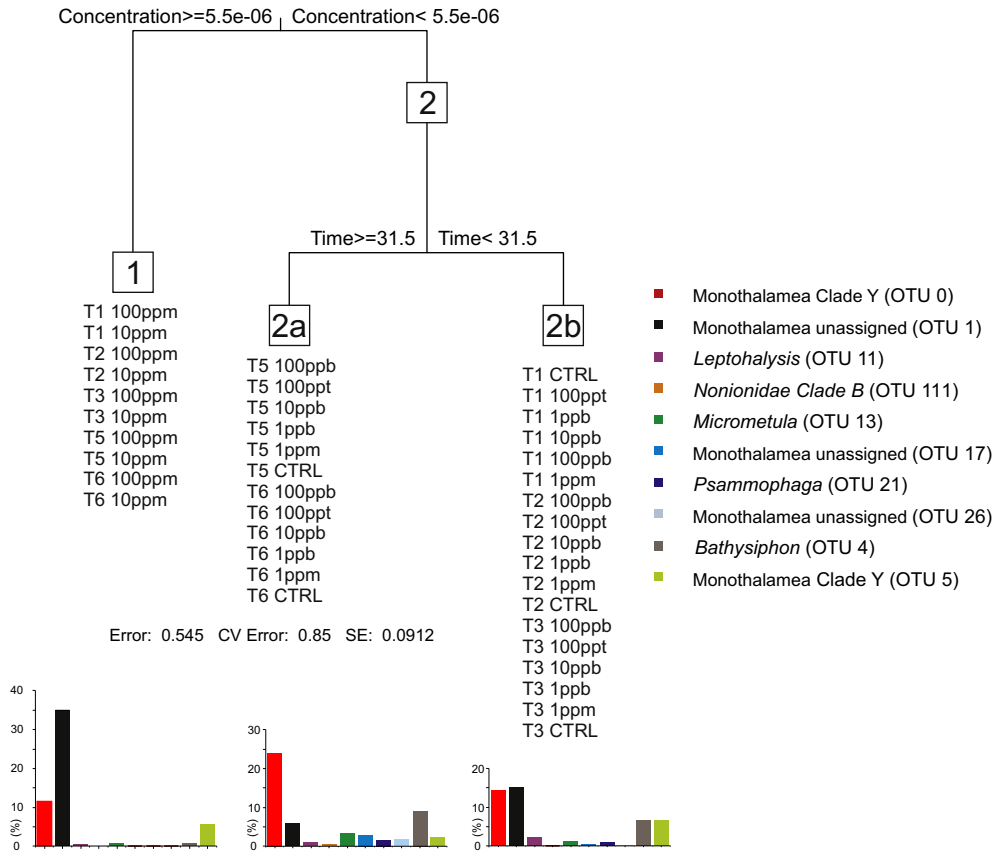

Fig. 5. Multivariate Regression Tree. Threshold values are reported at each node. The bar plots represent the mean relative abundances of OTUs per group. (For interpretation of the references to color in this figure legend, the reader is referred to the web version of this article.)

4.3. Foraminiferal eDNA indicators of Hg impact

A reduction in foraminiferal diversity (OTUs richness and Shannon diversity) in relation to anthropogenic stressors was observed in several metabarcoding studies based on eDNA and eRNA data. It has been related to lower redox mirroring the vicinity of the fish cages in Scotland (Pawlowski et al., 2014a) and associated with increasing enrichment stage (Pochon et al., 2015), following an index elaborated to qualify the health of the benthic ecosystems (Keeley et al., 2012). A significant correlation was also found between foraminiferal diversity indexes inferred from metabarcoding data and the distance from the oil wellheads (Laroche et al., 2016).

Our laboratory-experiment confirms the applicability of foraminiferal eDNA metabarcoding in environmental monitoring programs. In fact, similarly to field-based metabarcoding studies, a reduction of OTUs diversity (Shannon and Fisher α index) was observed in the mesocosm foraminiferal assemblages, particularly when Hg concentrations in sediments are considered. Additionally, some species like *Bathysiphon* (OTU 4), unassigned monothalamid (OTU 14), *Micrometula* (OTU 13), unassigned monothalamid (OTU 17), *Leptohalysis* (OTU 11), and *Psammophaga* (OTU 21) have been regarded as more sensitive to Hg increase than other taxa such as unassigned monothalamid (OTU 1), monothalamid Clade Y (OTU 5) and unassigned monothalamid (OTU 29). The opportunistic-like behaviors of these OTUs might result from the decline of other OTUs and competitors or from better adaptation to culture conditions.

However, any generalization about ecological tolerance of different foraminiferal species (OTUs) revealed by eDNA data should be considered with care. For instance, *Bathysiphon* and *Micrometula*, that appear quite sensitive in the present study, were correlated with more oxic conditions in Scotland (Pawlowski et al., 2014a; Pochon et al., 2015) and *Psammophaga* with intermediate stress conditions in New Zealand (Pochon et al., 2015) and opportunist towards organic matter in Adriatic Sea (Sabbatini et al., 2012). On the other hand, *Leptohalysis* that in our experiment seems to be particularly sensitive to Hg increase has been regarded as very tolerant to other stress such as increased organic matter content (Sabbatini et al., 2012; Pawlowski et al., 2014a; Pochon et al., 2015). Laroche et al. (2016) identified some OTUs decreasing in abundance from oil wellheads like *Bathysiphon* sp. 1 (OTU 32), unidentified globothalamids (OTUs 234 and 226) and monothalamid (OTU 313) whereas increasing abundances of *Reophax* sp. (OTU 23) and unidentified monothalamids (OTUs 73, 145 and 297) were associated at distal sites. Although with no statistical significance, the same authors reported very low abundances of *Nonion* sp. (OTU 115) and *Nemogullmia* sp. (OTU 95) in correspondence to the distance from the oil wellhead. Similarly, in our experiment Nonionidae (OTUs 44 and 111) and *Nemogullmia* sp. (OTU 25) are associated with low Hg concentrations. On the other hand, *Bathysiphon* (OTU 4) is commonly found at lower concentrations of Hg and its abundance is particularly low at Hg concentration over 10 ppm.

Interestingly, in an experiment to understand the response of benthic foraminifera to Cd, Pb, Hg and Zn, Brouillette (2009) reported *Psammophaga simplora* as able to withstand exposure to small concentrations of heavy metals but significantly reduced in all heavy metal treatments. In particular, no marked differences in *P. simplora* abundance between treatment (up to 3.6 ppm of Cd) and control were documented but when the Cd concentrations was increased to 10.36 ppm an acute response was observed.

4.4. Practical advantages and limitations of foraminiferal metabarcoding

This study reinforces the potential and the applicability of foraminiferal metabarcoding in environmental monitoring programs. In particular, the cost-effective, reliability, unneeded taxonomic expertise and rapid identification of foraminifera make the eDNA metabarcoding a valid methodology to process simultaneously and automatically

higher number of samples and is particularly adapted to large-scale biomonitoring (Pawlowski et al., 2014a). High numbers of reads are obtained even when small amount of sediment (< 2 g) is available, which ensures a proper statistical treatment. Furthermore, metabarcoding allows the consideration of soft-shelled taxa (monothalamids) or the very small foraminiferal species that for practical reasons are routinely discarded in the standard foraminiferal biomonitoring (Schönfeld et al., 2012).

Another practical advantage of eDNA metabarcoding is standardized identification of DNA sequences allowing automatic assignment of sequences to OTU, which can be easily compared between different studies. This removes the uncertainty related to the manual identification of species in a traditional morphology-based approach. It also allows distinguishing cryptic species that are common in practically all foraminiferal morphospecies (Pawlowski et al., 2008; Majewski et al., 2015). As shown in our study, the majority of these OTUs cannot be assigned taxonomically. Of course, the interpretation of observed patterns of OTUs distribution would be easier if it is assigned to particular morphospecies of known ecology, like in the case of *Virgulinella*. However, this would require special efforts to develop reference databases of DNA barcodes that would allow unambiguously assign OTUs to bioindicator species and facilitate the direct comparison with biomonitoring studies using conventional morphology-based metrics. Alternatively, the taxonomically unassigned species can be analyzed through taxonomy-free approaches, which provides OTU with ecological value based on known environmental parameters (Apothéloz-Perret-Gentil et al., 2017) or using machine learning methods to predict biotic indices (Cordier et al., 2017). In our study, the OTUs that dominate eDNA datasets in high Hg concentration do not need to be assigned taxonomically to become good candidates as bioindicators. In fact, their indicator value depends whether they will show the same patterns of occurrence in other eDNA-based studies of Hg polluted sediments.

For these reasons, the foraminiferal metabarcoding might represent a valuable tool for environmental biomonitoring and possibly a complement to standard morphological analyses. However, the metabarcoding approach has also some important limitations.

First, the eDNA dataset contains a lot of extracellular DNA molecules that are preserved in the sediments. The proportion of this “free” DNA fraction is difficult to evaluate especially that the analyzed dataset is a result of PCR amplification, which makes no distinction between active and inactive molecules. This issue can be partly overcome by using environmental RNA, which degradation is faster than DNA (Orsi et al., 2013; Laroche et al., 2017), or by using longer DNA fragments that are more difficult to be preserved as free molecules in the sediments. In our study, we address this issue by using a filter that removes all rare sequences present in < 10 reads, but it would be unfounded to claim that all remaining sequences correspond to living species, especially given a small volume of sediments, from which the eDNA was extracted. In the framework of future mesocosm experiments, it would be worth testing the influence of extracellular DNA on the analysis of diversity responses for biomonitoring, either towards the intensification of the ecological signal as the DNA of the large, positively-responding populations accumulates, or towards the spreading of a pan-genomic-DNA mixture exacerbating rarity patterns.

Another important limitation for routine application of eDNA surveys is the lack of validation studies that would confirm or infirm the observed patterns. Benthic monitoring of salmon farms is the only activity for which extensive material have been already collected and published (Pawlowski et al., 2014a, 2016; Lejzerowicz et al., 2015; Pochon et al., 2015). In the case of other activities, such as the oil and gas industry, only preliminary metabarcoding studies have been published (Laroche et al., 2016, 2017). For many other anthropogenic activities that have impact on marine ecosystem there is no published metabarcoding data yet.

Finally, the interpretation of eDNA metabarcoding data can also be hampered by some uncertainties related to the filtering and clustering of sequences (Flynn et al., 2015). In our study, we use filter that removes all sequences that are present in < 10 occurrences but any of such filters is arbitrary. OTU clustering is also based on some arbitrary parameters that may not reflect accurately genetic diversity of some foraminiferal species. In particular, the presence of intragenomic polymorphism in rRNA genes of many benthic foraminifera makes difficult the correct interpretation of these sequences (Pillet et al., 2012; Weber and Pawlowski, 2013).

Theoretically, all these limitations can be overcome by further studies focusing on increasing number of samples and more accurate data analysis. However, one information that eDNA metabarcoding studies are not able to provide is the description of morphological deformations of foraminiferal tests. Such deformations are often found in highly polluted environments and are commonly used as evidence for heavy metal pollution (Yanko et al., 1998). Our study is based on ribosomal RNA genes that are not involved in morphogenesis of foraminiferal test. From this perspective, the microscopic examination of foraminiferal assemblage remains the only valid way to assess the impact of pollution by mercury or other toxic compounds.

5. Conclusions

1- The mesocosm approach combined with molecular and standard morphological techniques proves to be an effective method to study benthic foraminiferal responses to various types and concentrations of pollutants over time.
2- The present study evidences that Hg pollution has detrimental effects on benthic foraminiferal diversity inferred from both morphological and molecular assemblages.
3- The use of Rose Bengal staining leads to overestimate of 30% the living foraminifera community compared to CTG.
4- Compared to morphological approach, the eDNA metabarcoding offers several advantages, such as wider range of analyzed taxa, including the monothalamids and some conspicuous hard-shelled species, among which some may be potential key foraminiferal (OTUs) indicators of Hg pollution.
5- Collectively, this study further supports the use of eDNA-based foraminiferal metabarcoding as a complementary and/or alternative method to biomonitoring program.

Supplementary data to this article can be found online at https://doi.org/10.1016/j.marpolbul.2017.10.022.

Acknowledgements

The research for this paper was made possible by the financial support from the PRIN 2010–2011 Ministero dell'Istruzione, dell'Università e della Ricerca (MIUR) (protocollo 2010RMTLYR) to RC. This study was supported by the Swiss National Science Foundation (grants 316030_150817 and 31003A_159709).

References

Alve, E., 1995. Benthic foraminiferal responses to estuarine pollution: a review. J. Foraminifer. Res. 25, 190–203.
Apothéloz-Perret-Gentil, L., Cordonier, A., Straub, F., Iseli, J., Esling, P., Pawlowski, J., 2017. Taxonomy-free molecular diatom index for high-throughput eDNA biomonitoring. Mol. Ecol. Resour. http://dx.doi.org/10.1111/1755-0998.12668.
Armynot du Châtelet, É., Debenay, J.P., 2010. The anthropogenic impact on the western French coasts as revealed by foraminifera: a review. Rev. Micropaleontol. 53, 129–137.
Baird, D.J., Hajibabaei, M., 2012. Biomonitoring 2.0: a new paradigm in ecosystem assessment made possible by next-generation DNA sequencing. Mol. Ecol. 21, 2039–2044.
Batrakova, N., Travnikov, O., Rozovskaya, O., 2014. Chemical and physical transformations of mercury in the ocean: a review. Ocean Sci. 10, 1047–1063.
Bernhard, J.M., Bowser, S.S., 1996. Novel epifluorescence microscopy method to determine life position of foraminifera in sediments. J. Micropalaeontol. 15, 68.
Bernhard, J.M., Ostermann, D.R., Williams, D.S., Blanks, J.K., 2006. Comparison of two

methods to identify live benthic foraminifera: a test between Rose Bengal and CellTracker Green with implications for stable isotope paleoreconstructions. Paleoceanography 21.
Brouillette, E., 2009. An experimental approach to understand the repose of benthic foraminifera to Cd, Pb, Hg and Zn. In: MSC Thesis. The University of Georgia, pp. 88.
Caruso, A., Cosentino, C., Tranchina, L., Brai, M., 2011. Response of benthic foraminifera to heavy metal contamination in marine sediments (Sicilian coasts, Mediterranean Sea). Chem. Ecol. 27, 9–30.
Ciacci, C., Canonico, B., Bilaničová, D., Fabbri, R., Cortese, K., Gallo, G., Marcomini, A., Pojana, G., Canesi, L., 2012. Immunomodulation by different types of N-oxides in the hemocytes of the marine bivalve *Mytilus galloprovincialis*. PLoS One 7 (5), e36937. http://dx.doi.org/10.1371/journal.pone.0036937.
Cimerman, F., Langer, M.R., 1991. Mediterranean foraminifera. In: Slovenska akademija znanosti in umetnosti, Ljubljana, (118 pp).
Coccioni, R., Frontalini, F., Marsili, A., Mana, D., 2009. Benthic foraminifera and trace element distribution: a case-study from the heavily polluted lagoon of Venice (Italy). Mar. Pollut. Bull. 59, 257–267.
Cordier, T., Esling, P., Lejzerowicz, F., Visco, J., Ouadahi, A., Martins, C., Cedhagen, T., Pawlowski, J., 2017. Predicting the ecological quality status of marine environments from eDNA metabarcoding data using supervised machine learning. Environ. Sci. Technol. http://dx.doi.org/10.1021/acs.est.7b01518.
Core Team, R., 2016. R: A Language and Environment for Statistical Computing. R Foundation for Statistical Computing, Vienna, Austria.
Creer, S., Fonseca, V.G., Porazinska, D.L., Giblin-Davis, R.M., Sung, W., Power, D.M., Packer, M., Carvalho, G.R., Blaxter, M.L., Lambshead, P.J., Thomas, W.K., 2010. Ultrasequencing of the meiofaunal biosphere: practice, pitfalls and promises. Mol. Ecol. 19, 4–20.
De'ath, G., 2002. Multivariate regression trees: a new technique for modeling species-environment relationships. Ecology 83, 1105–1117.
De'ath, G., 2014. mvpart: multivariate partitioning. In: R Package Version 1.6-2.
Di Leonardo, R., Bellanca, A., Capotondi, L., Cundy, A., Neri, R., 2007. Possible impacts of Hg and PAH contamination on benthic foraminiferal assemblages: an example from the Sicilian coast, central Mediterranean. Sci. Total Environ. 388, 168–183.
EPA 3052 protocol, 1996. SW-846 Test Method 3052: Microwave Assisted Acid Digestion of Siliceous and Organically Based Matrices.
Ernst, S.R., Morvan, J., Geslin, E., Le Bihan, A., Jorissen, F.J., 2006. Benthic foraminiferal response to experimentally induced Erika oil pollution. Mar. Micropaleontol. 61, 76–93.
Esling, P., Lejzerowicz, F., Pawlowski, J., 2015. Accurate multiplexing and filtering for high-throughput amplicon-sequencing. Nucleic Acids Res. 43, 2513–2524.
Ferraro, L., Sprovieri, M., Alberico, I., Lirer, F., Prevedello, L., Marsella, E., 2006. Benthic foraminifera and heavy metals distribution: a case study from the Naples Harbour (Tyrrhenian Sea, Southern Italy). Environ. Pollut. 142, 274–287.
Fiorini, F., Vaiani, S.C., 2001. Benthic foraminifers and transgressive-regressive cycles in the Late Quaternary subsurface sediments of the Po Plain near Ravenna (Northern Italy). Boll. Soc. Paleontol. Ital. 40, 357–403.
Fitzgerald, W.F., Lamborg, C.H., Hammerschmidt, C.R., 2007. Marine biogeochemical cycling of mercury. Chem. Rev. 107, 641–662.
Flynn, J.M., Brown, E.A., Chain, F.J., MacIsaac, H.J., Cristescu, M.E., 2015. Toward accurate molecular identification of species in complex environmental samples: testing the performance of sequence filtering and clustering methods. Ecol. Evol. 2252–2266.
Frontalini, F., Coccioni, R., 2008. Benthic foraminifera for heavy metal pollution monitoring: a case study from the central Adriatic Sea coast of Italy. Estuar. Coast. Shelf Sci. 76, 404–417.
Frontalini, F., Coccioni, R., 2011. Benthic foraminifera as bioindicators of pollution: a review of Italian research over the last three decades. Rev. Micropaleontol. 54, 115–127.
Frontalini, F., Coccioni, R., 2012. The response of the benthic foraminiferal community to copper exposure: the mesocosm experience. J. Environ. Prot. 3, 342–352.
Frontalini, F., Buosi, C., Da Pelo, S., Coccioni, R., Cherchi, A., Bucci, C., 2009. Benthic foraminifera as bio-indicators of trace element pollution in the heavily contaminated Santa Gilla lagoon (Cagliari, Italy). Mar. Pollut. Bull. 58, 858–877.
Frontalini, F., Coccioni, R., Bucci, C., 2010. Benthic foraminiferal assemblages and trace element contents from the lagoons of Orbetello and Lesina. Environ. Monit. Assess. 170, 245–260.
Frontalini, F., Curzi, D., Cesarini, E., Canonico, B., Giordano, F.M., De Matteis, R., Bernhard, J.M., Pieretti, N., Gu, B., Eskelsen, J., Jubb, A.M., Zhao, L., Pierce, E.M., Gobbi, P., Papa, S., Coccioni, R., 2016. Mercury-pollution induction of intracellular lipid accumulation and lysosomal compartment amplification in the benthic foraminifer ammonia parkinsoniana. PLoS One 11 (9), e0162401. http://dx.doi.org/10.1371/journal.pone.0162401.
Gentès, S., Maury-Brachet, R., Feng, C., Pedrero, Z., Tessier, E., Legeay, A., Mesmer-Dudons, N., Baudrimont, M., Maurice, L., Amouroux, D., Gonzalez, P., 2015. Specific effects of dietary methylmercury and inorganic mercury in zebrafish (*Danio rerio*) determined by genetic, histological, and metallothionein responses. Environ. Sci. Technol. 49, 14560–14569.
Gu, B., Bian, Y., Miller, C.L., Dong, W., Jiang, X., Liang, L., 2011. Mercury reduction and complexation by natural organic matter in anoxic environments. Proc. Natl. Acad. Sci. 108 (4), 1479–1483.
Gu, B., Mishra, B., Miller, C., Wang, W., Lai, B., Brooks, S.C., Kemner, K.M., Liang, L., 2014. X-ray fluorescence mapping of mercury on suspended mineral particles and diatoms in a contaminated freshwater system. Biogeosciences 11, 5259–5267.
Gustafsson, M., Dahllöf, I., Blanck, H., Hall, P., Molander, S., Nordberg, K., 2000. Benthic foraminiferal tolerance to tri-n-butyltin (TBT) pollution in an experimental mesocosm. Mar. Pollut. Bull. 40, 1072–1075.
Gworek, B., Bemowska-Kałabun, O., Kijeńska, M., Wrzosek-Jakubowska, J., 2016. Mercury in marine and oceanic waters—a review. Water Air Soil Pollut. 227, 371. http://dx.doi.org/10.1007/s11270-016-3060-3.
Hammer, Ø., Harper, D.A.T., Ryan, P.D., 2001. PAST: paleontological statistics software package for education and data analysis. Palaeontol. Electron. 4 (9pp).
Hines, N.A., Brezonik, P.L., 2004. Mercury dynamics in a small Northern Minnesota lake: water to air exchange and photoreactions of mercury. Mar. Chem. 90, 137–149.
Jorissen, F.J., 1988. Benthic foraminifera from the Adriatic Sea: principles of phenotypic variation. Utrecht Micropaleontol. Bull. 37, 1–174.
Keeley, N., Forrest, B., Crawford, C., Macleod, C., 2012. Exploiting salmon farm benthic enrichment gradients to evaluate the regional performance of biotic indices and environmental indicators. Ecol. Indic. 23, 453–466.
Kircher, M., Heyn, P., Kelso, J., 2011. Addressing challenges in the production and analysis of illumina sequencing data. BMC Genomics 12, 382. http://dx.doi.org/10.1186/1471-2164-12-382.
Lamborg, C.H., Hammerschmidt, C.R., Gill, G.A., Mason, R.P., Gichuki, S., 2012. An intercomparison of procedures for the determination of total mercury in seawater and recommendations regarding mercury speciation during GEOTRACES cruises. Limnol. Oceanogr. Methods 10, 90–100.
Laroche, O., Wood, S.A., Tremblay, L.A., Ellis, J.I., Lejzerowicz, F., Pawlowski, J., Lear, G., Atalah, J., Pochon, X., 2016. First evaluation of foraminiferal metabarcoding for monitoring environmental impact from an offshore oil drilling site. Mar. Environ. Res. 120, 225–235.
Laroche, O., Wood, S.A., Tremblay, L.A., Lear, G., Ellis, J.I., Pochon, X., 2017. Metabarcoding monitoring analysis: the pros and cons of using co-extracted environmental DNA and RNA data to assess offshore oil production impacts on benthic communities. PeerJ 5, e3347.
Legendre, P., Gallagher, E.D., 2001. Ecologically meaningful transformations for ordination of species data. Oecologia 129, 271–280.
Lejzerowicz, F., Esling, P., Pawlowski, J., 2014. Patchiness of deep-sea benthic foraminifera across the Southern Ocean: insights from high-throughput DNA sequencing. Deep-Sea Res. II Top. Stud. Oceanogr. 108, 17–26.
Lejzerowicz, F., Esling, P., Pillet, L., Wilding, T.A., Black, K.D., Pawlowski, J., 2015. High-throughput sequencing and morphology perform equally well for benthic monitoring of marine ecosystems. Sci Rep 5, 13932. http://dx.doi.org/10.1038/srep13932.
Loeblich Jr., A.R., Tappan, H., 1987. Foraminiferal Genera and Their Classification. Van Reinhold Company, New-York (970 pp).
Long, E.R., MacDonald, D.D., Smith, S.L., Calder, F.D., 1995. Incidence of adverse biological effects within ranges of chemical concentrations in marine and estuarine sediments. Environ. Manag. 19, 81–97.
Maccotta, A., Cosentino, C., Coccioni, R., Frontalini, F., Scopelliti, G., Caruso, A., 2016. Distribution of Cr and Pb in artificial sea water and their sorption in marine sediments: an example from experimental mesocosms. Environ. Sci. Pollut. Res. 23, 24068–24080.
Majewski, W., Bowser, S.S., Pawlowski, J., 2015. Widespread intra-specific genetic homogeneity of coastal Antarctic benthic foraminifera. Polar Biol. 38, 2047–2058.
Martins, M.V.A., Silva, F., Laut, L.L.M., Frontalini, F., Clemente, I.M.M.M., Miranda, P., Figueira, R., Sousa, S.H.M., Dias, J.M.A., 2015. Response of benthic foraminifera to organic matter quantity and quality and bioavailable concentrations of metals in Aveiro lagoon (Portugal). PLoS One 10 (2), e0118077. http://dx.doi.org/10.1371/journal.pone.0118077.
Mason, R.P., Choi, A.L., Fitzgerald, W.F., Hammerschmidt, C.R., Lamborg, C.H., Soerensen, A.L., Sunderland, E.M., 2012. Mercury biogeochemical cycling in the ocean and policy implications. Environ. Res. 119, 101–117.
Metzker, M.L., 2010. Sequencing technologies — the next generation. Nat. Rev. Genet. 11, 31–46. https://doi.org/10.1038/nrg2626.
Moss, J.A., McCurry, C., Schwing, P., Jeffrey, W.H., Romero, I.C., Hollander, D.J., Snyder, R.A., 2016. Molecular characterization of benthic foraminifera communities from the Northeastern Gulf of Mexico shelf and slope following the Deepwater Horizon event. Deep-Sea Res. I 115, 1–9.
Murray, J.W., 2006. Ecology and Applications of Benthic Foraminifera. Cambridge University Press, New York, pp. 426.
Nigam, R., Linshy, V.N., Kurtarkar, S.R., Saraswat, R., 2009. Effects of sudden stress due to heavy metal mercury on benthic foraminifer Rosalina leei: laboratory culture experiment. Mar. Pollut. Bull. 59, 362–368.
Oksanen, J., Guillaume Blanchet, F., Friendly, M., Kindt, R., Legendre, P., McGlinn, D., Minchin, P.R., O'Hara, R.B., Simpson, G.L., Solymos, P., Stevens, M.P., Szoecs, E., Wagner, H., 2016. Vegan: community ecology package. In: R Package Version. 2. pp. 3–5.
Orsi, W., Biddle, J.F., Edgcomb, V., 2013. Deep sequencing of subseafloor eukaryotic rRNA reveals active fungi across marine subsurface provinces. PLoS One 8 (2), e56335. http://dx.doi.org/10.1371/journal.pone.0056335.
Pawlowski, J., Lecroq, B., 2010. Short rDNA barcodes for species identification in foraminifera. J. Eukaryot. Microbiol. 57, 197–205.
Pawlowski, J., Fahrni, J.F., Brykczynska, U., Habura, A., Bowser, S.S., 2002. Molecular data reveal high taxonomic diversity of allogromiid foraminifera in explorers cove (McMurdo Sound, Antarctica). Polar Biol. 25, 96–105.
Pawlowski, J., Majewski, W., Longet, D., Guiard, J., Cedhagen, T., Gooday, A.J., Korsun, S., Habura, A.A., Bowser, S.S., 2008. Genetic differentiation between Arctic and Antarctic monothalamous foraminiferans. Polar Biol. 31, 1205–1216.
Pawlowski, J., Fontaine, D., da Silva, A.A., Guiard, J., 2011. Novel lineages of Southern Ocean deep-sea foraminifera revealed by environmental DNA sequencing. In: Deep-sea Research Part II: Topical Studies in Oceanography. 58. pp. 1996–2003.
Pawlowski, J., Audic, S., Adl, S., Bass, D., Belbahri, L., Berney, C., et al., 2012. CBOL Protist working group: barcoding eukaryotic richness beyond the animal, plant, and fungal kingdoms. PLoS Biol. 10 (11), e1001419. http://dx.doi.org/10.1371/journal.pbio.1001419.

Pawlowski, J., Esling, P., Lejzerowicz, F., Cedhagen, T., Wilding, T.A., 2014a. Environmental monitoring through protist next-generation sequencing metabarcoding: assessing the impact of fish farming on benthic foraminifera communities. Mol. Ecol. Resour. 14 1129–114.

Pawlowski, J., Lejzerowicz, F., Esling, P., 2014b. Next-generation environmental diversity surveys of foraminifera: preparing the future. Biol. Bull. 227, 93–106.

Pawlowski, J., Lejzerowicz, F., Apothéloz-Perret-Gentil, L., Visco, J., Esling, P., 2016. Protist metabarcoding and environmental biomonitoring: time for change. Eur. J. Protistol. 55, 12–25.

Pillet, L., Fontaine, D., Pawlowski, J., 2012. Intra-genomic ribosomal RNA polymorphism and morphological variation in *Elphidium macellum* suggests inter-specific hybridization in foraminifera. PLoS One 7.

Pochon, X., Wood, S.A., Keeley, N.B., Lejzerowicz, F., Esling, P., Drew, J., Pawlowski, J., 2015. Accurate assessment of the impact of salmon farming on benthic sediment enrichment using foraminiferal metabarcoding. Mar. Pollut. Bull. 100, 370–382.

Sabbatini, A., Bonatto, S., Bianchelli, S., Pusceddu, A., Danovaro, R., Negri, A., 2012. Foraminiferal assemblages and trophic state in coastal sediments of the Adriatic Sea. J. Mar. Syst. 105-108, 163–174.

Saraswat, R., Kurtarkar, S.R., Mazumder, A., Nigam, R., 2004. Foraminifers as indicators of marine pollution: a culture experiment with *Rosalina leei*. Mar. Pollut. Bull. 48, 91–96.

Schönfeld, J., Alve, E., Geslin, E., Jorissen, F., Korsun, S., Spezzaferri, S., Abramovich, S., Almogi-Labin, A., du Chatelet, E.A., Barras, C., Bergamin, L., Bicchi, E., Bouchet, V., Cearreta, A., Di Bella, L., Dijkstra, N., Disaro, S.T., Ferraro, L., Frontalini, F., Gennari, G., Golikova, E., Haynert, K., Hess, S., Husum, K., Martins, V., McGann, M., Oron, S., Romano, E., Sousa, S.M., Tsujimoto, A., 2012. The FOBIMO (FOraminiferal BIoMOnitoring) initiative-towards a standardised protocol for soft-bottom benthic foraminiferal monitoring studies. Mar. Micropaleontol. 94-95, 1–13.

Scopelliti, G., Di Leonardo, R., Tramati, C.D., Mazzola, A., Vizzini, S., 2015. Premature aging in bone of fish from a highly polluted marine area. Mar. Pollut. Bull. 97, 333–341.

Stankovic, S., Kalaba, P., Stankovic, A.R., 2014. Biota as toxic metal indicators. Environ. Chem. Lett. 12, 63–84.

Ung, C.Y., Lam, S.H., Hlaing, M.M., Winata, C.L., Korzh, S., Mathavan, S., Gong, Z., 2010. Mercury-induced hepatotoxicity in zebrafish: in vivo mechanistic insights from transcriptome analysis, phenotype anchoring and targeted gene expression validation. BMC Genomics 11 (1), 212.

Visco, J.A., Apothéloz-Perret-Gentil, L., Cordonier, A., Esling, P., Pillet, L., Pawlowski, J., 2015. Environmental monitoring: inferring the diatom index from next-generation sequencing data. Environ. Sci. Technol. 49 (13), 7597–7605.

Weber, A.A.T., Pawlowski, J., 2013. Can abundance of protists be inferred from sequence data: a case study of foraminifera. PLoS One 8.

Wood, S.A., Smith, K.F., Banks, J.C., Tremblay, L.A., Rhodes, L., Mountfort, D., Cary, S.C., Pochon, X., 2013. Molecular genetic tools for environmental monitoring of New Zealand's aquatic habitats - past, present and the future. N. Z. J. Mar. Freshw. Res. 47, 90–119.

Yanko, V., Ahmad, M., Kaminski, M., 1998. Morphological deformities of benthic foraminiferal tests in response to pollution by heavy metals: implications for pollution monitoring. J. Foraminifer. Res. 28, 177–200.